



UNIVERSITI
MALAYSIA
KELANTAN

FYP FBKT

**CHARACTERIZATION OF Al_2O_3 - TiO_2 -EGGSHELL
NANOCOMPOSITE PREPARED BY HIGH ENERGY
BALL MILLING**

**Tan Hee Hong
J20A0635**

**A reported submitted in fulfilment of the requirements for the
degree of Bachelor of Applied Science (Material Technology)
with Honours**

**FACULTY OF BIOENGINEERING AND TECHNOLOGY
UMK**

2024

DECLARATION

I declare that this thesis entitled “Characterization of Al₂O₃-TiO₂-Eggshell Nanocomposite Prepared by High Energy Ball Milling” is the results of my own research except as cited in the references.

Signature : _____

Student's Name : _____

Date : _____

Verified by:

Signature : _____

Supervisor's Name : _____

Stamp : _____

Date : _____

ACKNOWLEDGEMENT

Firstly, I would like to express my gratitude to the authority of Faculty of Bioengineering and Technology for giving me this opportunity to finish my research for the final year project and for providing me with the laboratory and equipment.

Next, I would like to acknowledge Dr Mahani Yusoff as my supervisor for her guidance for me to finish this thesis and always open whenever I ran into trouble with my research writing or had a question. I would also like to thank Puan Hanisah and Cik Izzati in helping my characterization procedure easier and to En Qamal as lab assistant that take care my final year project team during midsem break. Special thanks to all lecturers and staff who had helped me directly or indirectly throughout completing my final year project.

My profound gratitude to my beloved parents with their unfailing support and continuous encouragement throughout the years of my study. Finally, thanks to my final year project team Danial, Aisyah, that stayed together, and this accomplishment is not possible without them. Thank you. I want to say thank you to my friend which is Chee Yu Cheng, Chong Guo Xian and others that always provide me with materials to help me complete my final year project.

UNIVERSITI
MALAYSIA
KELANTAN

Characterization of Al₂O₃-TiO₂-Eggshell Nanocomposite Prepared by High Energy Ball Milling

ABSTRACT

This study aimed to enhance the properties of Al₂O₃ matrix composite, addressing issues such as low toughness, ductility, and instability for high-temperature applications. Titanium dioxide (TiO₂) was chosen as a reinforcement due to its excellent chemical and mechanical stability, along with good compatibility with Al₂O₃. However, TiO₂ still had drawbacks. Hence, the addition of eggshell was explored to understand its effect on the Al₂O₃-TiO₂ nanocomposite. The Al₂O₃-TiO₂-Eggshell nanocomposite was fabricated through a simple and cost-effective method, powder metallurgy. Eggshells were cleaned, dried in an oven for 24 hours, and ground into powder. Alumina (Al₂O₃), titania (TiO₂), and eggshell powder (CaCO₃) were milled in a planetary ball mill using 5 mm zirconia balls at 300 rpm for varying durations of 5, 10, 15, and 20 hours. Subsequently, the composition was characterized using X-Ray Diffraction (XRD), Scanning Electron Microscope (SEM), and Fourier-Transform Infrared Spectroscopy (FTIR). The XRD analysis revealed no detectable phases for Al₂O₃, TiO₂, and CaCO₃. However, after 20 hours of milling, TiO₂ deposition covering the surface of CaCO₃ was observed. The milled composite powder was analyzed using the Williamson Hall method to calculate crystallite size and internal strain. Longer milling times resulted in a more refined structure and increased internal strain in the ball-mounted Al₂O₃-TiO₂-Eggshell composite. FTIR results exhibited the functional groups of the Al₂O₃-TiO₂-Eggshell composite, with detectable changes at 300 rpm as milling time increased. This suggests a modification in the composite's chemical composition or structure. Overall, the study demonstrates the potential of eggshell inclusion in improving the properties of Al₂O₃-TiO₂ nanocomposites, with implications for enhancing their suitability for high-temperature applications.

Keywords: Al₂O₃-TiO₂, Eggshell, Ceramic matrix nanocomposite, High energy milling, Milling time

Kajian nanokomposit Al₂O₃-TiO₂-Kulit Telur yang disediakan melalui

Pengisaran Bola Tenaga Tinggi.

ABSTRAK

Kajian ini dijalankan untuk menambahbaik sifat aplikasi Al₂O₃ seperti kekurangan Kekuatan, kemuluran dan juga ketidakstabilan untuk digunakan untuk aplikasi suhu tinggi. Pemilihan untuk TiO₂ sebagai tetulang adalah kerana kimia yang sangat baik, kestabilan mekanikal dan mempunyai keserasian yang baik dengan Al₂O₃ tetapi masih mempunyai kelemahan. Jadi, penambahan kulit telur adalah ingin mengetahui kesan kepada nanokomposit Al₂O₃-TiO₂. Nanokomposit Al₂O₃-TiO₂-Kulit Telur telah disediakan menggunakan kaedah yang mudah dan murah iaitu metalurgi serbuk kulit telur. akan dibersihkan dan dikeringkan di dalam ketuhar selama 24 jam dan kemudian dikisar dalam bentuk serbuk. Element alumina (Al₂O₃), titania (TiO₂) dan serbuk kulit telur (CaCO₃) dikisar dalam pengisar bola planet menggunakan bola zirconia 5 mm pada 300 rpm dan 5,10,15,20 jam. Kemudian, komposisi akan dicirikan oleh X-ray difraksi (XRD), Pengimbasan mikroskop eleftron (SEM) dan Spektroskopi inframerah fourier transformasi Fourier (F-TIR). Keputusan XRD menunjukkan tiada fasa telah dikesan untuk Al₂O₃, TiO₂ dan CaCO₃ tetapi dalam masa pengilangan 20h, terdapat fasa yang telah dikesan dimana pemendapan TiO₂ meliputi permukaan CaCO₃. Serbuk komposit yang dikisar ditentukan menggunakan kaedah Williamson Hall untuk mengira saiz kristal. dan terikan dalaman. Peningkatkan masa pengisaran menghasilkan lebih halus dan dipasang bola Al₂O₃-TiO₂- kulit telur apabila terikan dalaman meningkat. Hasil F-TIR menunjukkan kumpulan berfungsi kulit telur Al₂O₃-TiO₂ dan boleh dikesan pada 300 rpm apabila pengilangan masa bertambah.

Kata kunci: Al₂O₃- TiO₂, kulit Telur, Nanokomposit matriks seramik, Pengilangan tenaga tinggi, Masa pengilangan

TABLE OF CONTENT

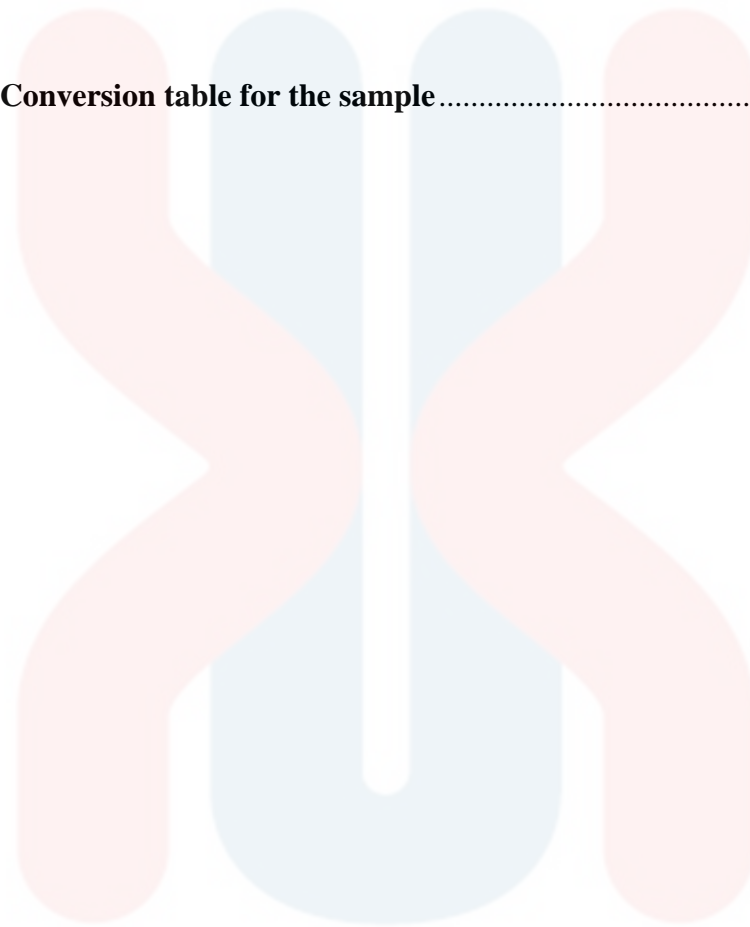
DECLARATION	ii
ACKNOWLEDGEMENT	iii
Characterization of Al ₂ O ₃ -TiO ₂ -Eggshell Nanocomposite Prepared by High Energy Ball Milling	iv
Kajian nanokomposit Al ₂ O ₃ -TiO ₂ -Kulit Telur yang disediakan melalui Pengisaran Bola Tenaga Tinggi.	v
TABLE OF CONTENT	vi
LIST OF TABLES	ix
LIST OF FIGURES	x
LIST OF ABBREVIATIONS (optional)	xi
LIST OF SYMBOLS (optional)	xii
CHAPTER 1	1
INTRODUCTION	1
1.1 Background of Study	1
1.2 Problem Statement.....	2
1.3 Objectives	3
1.4 Scope of Study.....	3
1.5 Significances of Study	3
CHAPTER 2	5

LITERATURE REVIEW	5
2.1 Ceramic Matrix Nanocomposite.....	5
2.1.1 Alumina-Based Composites	6
2.1.2 Natural filler in Nanocomposites.....	7
2.1.3 Type of Natural Filler	8
2.1.4 Eggshell as Natural Filler	8
2.1.5 Interaction Interfacial and Mechanical Properties	9
2.1.6 Preparation Technique of Al ₂ O ₃ -TiO ₂ -ES Nanocomposite	10
CHAPTER 3	11
MATERIALS AND METHODS.....	11
3.1 Introduction	11
3.2 Raw Material	12
3.3 Composition Preparation	12
3.3.1 Preparation of the eggshell powder	14
3.3.2 High Energy Milling.....	14
3.4 Characterisation of Al ₂ O ₃ -TiO ₂ -ES Nanocomposites	16
3.4.1 X-Ray Diffraction (XRD).....	16
3.4.2 Fourier -Transform Infrared Spectroscopy (F-TIR)	17
CHAPTER 4	18
RESULTS AND DISCUSSION	18
4.1 Raw Material	18
4.1.1 Phase Identification	18

4.1.2	Functional Group	20
4.2	Al ₂ O ₃ -TiO ₂ -ES Nanocomposite	21
4.2.1	Phase Identification	21
4.2.2	Crystallite size and internal strain.....	22
4.2.3	Functional group	24
4.3	Morphology	27
CHAPTER 5		29
CONCLUSIONS AND RECOMMENDATIONS		29
5.1	Conclusions	29
5.2	Recommendations	29
REFERENCES		31
APPENDIX A.....		34
APPENDIX B		35
APPENDIX C		36

LIST OF TABLES

Table 3.1: Conversion table for the sample.....	13
--	-----------



UNIVERSITI
MALAYSIA
KELANTAN

LIST OF FIGURES

Figure 3.1: Overall experiment in this study	11
Figure 3.2: Oven	14
Figure 3.3: High energy planetary ball mill.....	15
Figure 4.1: XRD pattern of the raw material Al_2O_3 , TiO_2 , ES	19
Figure 4.2: FTIR pattern of the raw material eggshell	20
Figure 4.3: XRD pattern of the milled powder mixture for a)2.5wt%-5h, b)2.5wt%-20h, c)15wt%-5h and 15wt%-20h milled at 300 rpm.....	21
Figure 4.4: Plot of $B_r \cos \theta$ against $\sin \theta$ for calculating Al_2O_3 crystallite size and internal strain at different ES compositions and milling time using WH method	22
Figure 4.5: Crystallite size and internal strain of the milled powder with different ES composition and milling times.....	23
Figure 4.6: FTIR pattern of the milled powder mixture at the different composition for 10h milling time.....	25
Figure 4.7: FTIR pattern of the milled powder mixture at the different ES composition milled for 20h.....	26
Figure 4.8: SEM images of Al_2O_3 – TiO_2 – Eggshell powder milled at (a)2.5wt%-5h (b)2.5wt%-20h (c)15wt%-5h (d)15wt%-20h at 300 rpm at 500x magnification	28

LIST OF ABBREVIATIONS (optional)

CMNC	Ceramic Matrix Nanocomposite
Al ₂ O ₃	Alumina
TiO ₂	Titania
ES	Eggshell
CaCO ₃	Calcium Carbonate
SiO ₂	Silicate
S	Sulfur
P	Phosphorus
Cl	Chlorine
Cr ₂ O ₃	Chromium (III) Oxide
MnO	Manganese (II) Oxide
Zn-Al	Zinc Aluminium
XRD	X-ray Diffraction
SEM	Scanning Electron Microscope
F-TIR	Fourier – transform infrared spectroscopy
PP	Polypropylene
COD	Crystallography Open Database
BET	Brunauer – Emmett – Teller

LIST OF SYMBOLS (optional)

B_{Cryst}	Broadening due to crystallite Size
B_i	Instrumental broadening
B_o	Sum of the total broadening of size, lattice strain and instrument
B_r	Overall broadening
B_{strain}	Broadening due to strain
h	Hours
m	mass
nm	nanometre
mm	millimetre
cm^{-1}	Reciprocal centimetre
rpm	Rotate per minute
wt%	Weight percent
μm	Micrometre
%	Percent
°	Degree
Θ	Theta
x	Time

CHAPTER 1

INTRODUCTION

1.1 Background of Study

Ceramic matrix nanocomposites (CMNCs) are a type of advanced material that is made up of a ceramic matrix that is reinforced with nanoparticles. The ceramic matrix can be made of a variety of materials such as oxides, carbides, nitrides, and borides. Carbon, silicon carbide, and alumina are examples of reinforcing materials. CMNCs are typical ceramic materials in terms of strength, stiffness, and toughness as well as resistance to high temperatures and wear. These materials are employed in a range of high-performance applications, including aircraft components, turbine blades, and spacecraft heat shields. Because of their features, they have potential use in various areas such as automotive and energy.

Alumina-titania ($\text{Al}_2\text{O}_3\text{-TiO}_2$) nanocomposite is a CMNC utilized in coating because of its excellent toughness, low thermal expansion, and low thermal conductivity. These characteristics make the $\text{Al}_2\text{O}_3\text{-TiO}_2$ nanocomposite a suitable material for construction and coatings in high-performance applications requiring heat barriers. Because of its features such as high toughness, low thermal expansion, and low thermal conductivity, alumina-titania ($\text{Al}_2\text{O}_3\text{-TiO}_2$) nanocomposite is utilized in coating. These characteristics make the $\text{Al}_2\text{O}_3\text{-TiO}_2$ nanocomposite a suitable material for construction and coatings in high-performance applications requiring heat barriers (Pinzón et al., 2018). $\text{Al}_2\text{O}_3\text{-TiO}_2$ coatings are ideal options for abrasive wear prevention because they are resistant to high-temperature erosion and have cryogenic compatibility. When TiO_2 is added to Al_2O_3 , the thermal shock resistance increases, the wear resistance increases, the adhesion strength increases, and the toughness of the coating improves without affecting the hardness. This increases the performance of the coating.

The hybrid CMNCs can be made by adding natural filler such as eggshell (ES). The ES is made up of 95% calcite calcium carbonate and 3.5% proteins, proteoglycans,

and glycoproteins. The cuticle is the ES's outermost layer, measuring 10-30 micrometers in thickness and being insoluble in water. The cuticle layer is made up of an organic layer that contains up to 90% protein and high quantities of cysteine, glycine, glutamic acid, lysine, and tyrosine. The composition of the eggshell consists of around 95% calcium carbonate in the form of calcite and 5% organic material such as Al_2O_3 , SiO_2 , S, P, Cl, and Cr_2O_3 , MnO sulphated polysaccharides, X collagen, and other proteins. Chicken eggshell is frequently utilized because of its mass availability, lightweight, low cost, and environmental friendliness (Sunardi et al., 2023). The ES is quietly use in the composite such as the polymer composite as a reinforcer . Some of the work is carryout that the ES is using as the new material on the polymer composites which is new bio-filler for polypropylene composites (Hassan et al., 2012). ES has a lesser density than the mineral calcium carbonate. The ES will be used to demonstrate strong interfacial connections with different matrices. For example, in the Zn–Al alloy, the addition of the ES for 20 % vol just increases the elongation and tensile strength. For the small summary, the adhesion between the filler and matrix might be improved by a large energy differential between the ES surface and the matrix.

Even the Al_2O_3 - TiO_2 nanocomposite combines to improve their own great properties, but this material still has limitations. Therefore, the development of Al_2O_3 - TiO_2 nanocomposite will be focused on the use of natural filler to enhance the properties of nanocomposites and why the natural filler was chosen.

1.2 Problem Statement

The Al_2O_3 - TiO_2 nanocomposite performs great properties such as better mechanical, thermal, and chemical characteristics. However, there are still limitations for this material like limited compatibility because of different crystal structures and thermal expansion coefficients. This can lead to difficulties in achieving a homogeneous distribution of the two nanoparticles within the composite, which can affect the overall material properties and the cost that needs to produce the Al_2O_3 - TiO_2 nanocomposite contributing to the overall high cost of production. Thus, the involvement of natural fillers can reduce the cost because natural fillers are generally abundant, renewable, and cost-effective compared to synthetic fillers. Incorporating natural fillers into alumina-titania

nanocomposites can help reduce the overall cost of production. The advantages of the hybrid composite are not only reduced cost but also can improve mechanical properties, synergistic effects, and increased damage resistance.

1.3 Objectives

The objectives of this research are:

1. To synthesize the Al_2O_3 - TiO_2 -ES nanocomposite at different milling times and composition using high energy ball milling,
2. To evaluate the structural, morphology, and physical properties of the milled Al_2O_3 - TiO_2 -ES nanocomposite.

1.4 Scope of Study

This study focusses on the effect of mixing the chicken eggshell into Al_2O_3 - TiO_2 nanocomposite by characterizing the milling time and composition of the ES in Al_2O_3 - TiO_2 nanocomposite sample by the constant milling. Characterization technique that involving in this study are X- Ray Diffraction (XRD) and Scanning Electron Microscope (SEM) for the phase identification and morphology, and Fourier-transform infrared spectroscopy (FTIR) to identify the compound of the nanocomposite.

1.5 Significances of Study

Al_2O_3 - TiO_2 nanocomposite was the greatest material with high hardness and tensile strength. The aim of this research is to find out the use of a natural filler such as eggshell to perform the hybrid composite and for further study on the characterization of

$\text{Al}_2\text{O}_3\text{-TiO}_2\text{-ES}$ nanocomposite with the parameter prepared by a combined mechanical technique.



UNIVERSITI
MALAYSIA
KELANTAN

CHAPTER 2

LITERATURE REVIEW

2.1 Ceramic Matrix Nanocomposite

Composites are the materials that compose two or more two with dissimilar chemical or physical properties to become a better distinction material from their individual unit. The nanocomposite materials are like micro composites. They are composed of two or more materials, but the difference is the size of the composite is larger than 100 nanometers. Compared to the advantage of the micro composite, the nanocomposite is better at increasing strength, stiffness, and thermal stability due to its unique properties. Nanocomposites are used in various fields, including aerospace, automotive, electronics, and biomedical engineering. In addition, due to their unique properties, nanocomposite materials are often preferred for applications where high performance and durability are required, such as structural materials, coatings, and sensors (Meneghetti & Qutubuddin, 2006).

Nanocomposites can be made from the main class of materials such as polymer, metal, and ceramic. Among these materials, polymer is the most popular and studied nanocomposite among researchers. Ceramics are recognized for their better thermal stability and strength than metals and polymers, but their fundamental restriction is brittleness. As a result, ceramic matrix nanocomposites (CMNNs) are being employed to increase composite toughness which enables them to be used in high-temperature applications. Recently, the development of CMNCs can be multiphase ceramic or single-phase ceramic either oxide or no-oxide as the matrix combining with the reinforcing factor Based on the benefits of CMNCs they may be used in industries such as cutting tools, aircraft, energy, biomedical engineering, electronic applications, and environmental applications with excellent non-degradation properties(Rathod et al., 2017).

2.1.1 Alumina-Based Composites

Alumina (Al_2O_3) is a high thermal conductivity aluminium and oxygen combination that is commonly utilized as an electrical insulator. It possesses great hardness, compressive strength, chemical and thermal stability. However, due to its low fracture toughness and strength, its application as a structural material has been limited. Lack of these properties makes them easily prone to fractures, resulting the unexpected failure during service(Karadimas & Salonitis, 2023).

Reinforcing Al_2O_3 with titanium oxide (TiO_2) has been developed as a coating material as a result they are able to offer excellent abrasion resistance in high temperature applications (Kim & Lee, 1989). TiO_2 has excellent wear resistance and chemical inertness. The influence of dispersion of TiO_2 particle in Al_2O_3 matrix gives a significant effect on wear resistance, coating strength, and toughness of the composite. However, the total amount of TiO_2 particles in Al_2O_3 must have an optimum value because they are very sensitive to composites mechanical properties. Al_2O_3 - TiO_2 micro composite and nanocomposite have long been used as coating materials. However, Al_2O_3 - TiO_2 composite suffers from inherent surface defects(Sharma et al., 2001). In the matrix, tight interfacial bonding between the Al_2O_3 matrix and TiO_2 and thus led to a good stress transfer within the composite. Ceramic is still more brittle than metals because of its own material limitations.

This composite could be added with another the ceramic filler. These are called ceramic hybrid nanocomposites. The ceramic filler can be in type of synthetic or natural filler. The addition of natural filler could become a promising approach to minimizing the problem of environmental pollution. The use of these sorts of fillers as reinforcing components in polymer composites is an efficient technique to create environmentally benign and naturally degradable composites without compromising their stiffness(Zaaba & Ismail, 2019). The effect of filler amount in hybrid Al_2O_3 composite has been studied less so far in literature.

2.1.2 Natural filler in Nanocomposites

Natural filler is the material that is derived from renewable material, such as plants, animals or mineral that can be incorporated in the composite material to enhance their properties. Compared to synthetic filler, a natural filler has offered several advantages such cost effectiveness, sustainability, and compatibility with the various material.

Cellulose is the most prevalent natural polymer, and it has certain distinct qualities such as ease of availability, renewability, lightweight, and environmental friendliness. (Roy et al., 2021). The stiffness, tensile strength, and impact resistance of composite materials can all be enhanced by cellulosic fillers. They are frequently utilized in applications for packaging, building materials, automotive components, and polymer composites.

Mineral filler is the material which is the fine pulverized inert mineral or rock that is included in the manufactured products such as paper, rubber, and plastic. The effect of the mineral filler can enhance the composite properties such as high thermal stability, chemical inertness, and low cost. An example of minerals is calcium carbonate, talc, wollastonite, and silica which is usually used in the plastic factory. They can improve properties such as dimensional stability, flame retardancy, hardness and impact strength.(Jang, 2016)

Due to their environmental sensitivity and availability as renewable resources, bio-based fillers have found major uses and have the potential to be utilized as fillers. Additional attractive features of natural fiber-based polymer composites are low cost, good mechanical and heat resistance, biodegradability, and environmental friendliness. It has also been discovered that biocomposites reduce costs while enhancing their mechanical, thermal, and rheological properties. To further improve the characteristics of polymer composites, hybrid composites were created by combining particles and short fibres in a single matrix. Using traditional processes such as extrusion compounding and injection moulding, particles and short fibres may be directly introduced into thermoplastics.(Essabir et al., 2016)

Animal-based filler is the material that we can get from waste such as eggshell, keratin from feathers and chitosan from crustacean shells. These fillers have a unique property, and they can provide the specific functionalities to the composite's application based on their own properties. These fillers are mostly applied in medical applications.

2.1.3 Type of Natural Filler

Plants are the source of natural fibre, which includes jute, flax, bamboo, coir, kenaf, and sisal. These fillers have great mechanical qualities, such as high strength, stiffness, and specific modulus. Natural fibre composites are used in consumer items, furnishings, construction materials, and automotive components. To strengthen the composite matrix, the fibres might be woven into mats, employed as short fibres, or as long, continuous fibres, because of these properties, Natural fiber-based polymeric composites have combination qualities such as good insulation and high levels of desired mechanical strength, allowing them to be great mechanical supports for field carrying conductors (Paul et al., 2021) . These distinct qualities enable such composites to be employed in a wide range of applications, including terminals, connections, printed circuit boards, switches, insulators, industrial and domestic plugs, panels, and so on. (Al-Oqla et al., 2015).

Materials like calcium carbonate, talc, mica, kaolin, and silica are examples of mineral fillers. Calcium carbonate (CaCO_3) is the mineral filler that is most frequently used in plastic, notably polypropylene (PP). This kind of filler is affordable and suitable for usage at high filler levels. According to reports, sheet-like platy fillers like mica, talc, and kaolin increase stiffness (Nurdina et al., 2009).

2.1.4 Eggshell as Natural Filler

Due to its distinct composition and characteristics, the eggshell has the potential to serve as a filler for alumina-titanium ($\text{Al}_2\text{O}_3\text{-TiO}_2$) nanocomposite. The main components of eggshells (ES), a byproduct of the chicken business, are CaCO_3 and organic substances. To improve the mechanical and functional qualities of different composite materials, it has been investigated as a filler. The ES is made up of 3.5% protein, proteoglycans, glycoproteins, and the calcite form for 95% of calcium carbonate. The cuticle, which has a thickness of 10 to 30 μm and is insoluble in water, is the ES's

outermost coat. The organic cuticle layer has a high concentration of cysteine, glycine, glutamic acid, lysine, and tyrosine and can include up to 90% protein. (Hassan & Aigbodon, 2015) claim that the ES particles' significantly affects the tensile strength.

2.1.5 Interaction Interfacial and Mechanical Properties

The components of the eggshell such as proteins, proteoglycans, and glycoproteins, for example, can form chemical bonds with the alumina and titania phases in the matrix. Organic functional groups in eggshell, like amino, carboxyl, and hydroxyl groups, can react with surface functional groups on alumina and titania nanoparticles, generating covalent or hydrogen bonding at the interface. These chemical linkages facilitate load transmission and generate strong adhesion between the eggshell and the ceramic matrix. Interfacial adhesion can also be influenced by van der Waals forces and electrostatic interactions between the surfaces of the eggshell and the alumina-titania matrix. Physical interactions can improve mechanical interlocking at the interface by facilitating tight contact between the two phases. Physical elements that can prevent delamination or debonding at the contact include hydrogen bonding, dipole-dipole interactions, and London dispersion forces. (Vandeginste, 2021). During the production process, the uneven surface morphology of eggshell particles, together with their distinct microstructure, might cause mechanical interlocking with the alumina-titania matrix. The eggshell particles may become embedded in the ceramic matrix, forming a strong mechanical interlock between the two phases. Mechanical interlocking improves load transfer and crack propagation resistance, boosting the mechanical characteristics of the nanocomposite.

2.1.6 Preparation Technique of Al_2O_3 - TiO_2 -ES Nanocomposite

Techniques like mechanical alloying, powder metallurgy, or electrodeposition are frequently used to fabricate ceramic-based nanocomposites. These techniques make it possible for fillers to be evenly distributed throughout the ceramic matrix, ensuring that the reinforcements are distributed uniformly and producing a suitable composite structure. Mechanical alloying that uses high energy ball milling could be to produce Al_2O_3 - TiO_2 -ES nanocomposite. This method creates surface diffusion as well as a uniform dispersion of reinforced material for creating ceramic-matrix nanocomposites. Powders are milled under particular circumstances that bring tremendous energy into the system, substantially lowering the original average particle size, resulting in extremely small particles with crystallite sizes in the nanometer range and homogenous, intimately mixed powders during the milling process (Alves et al., 2020).

CHAPTER 3

MATERIALS AND METHODS

3.1 Introduction

This research focuses on the production and characterisation of the nanocomposite. Figure 3.1 depicts the complete experiment for this research.

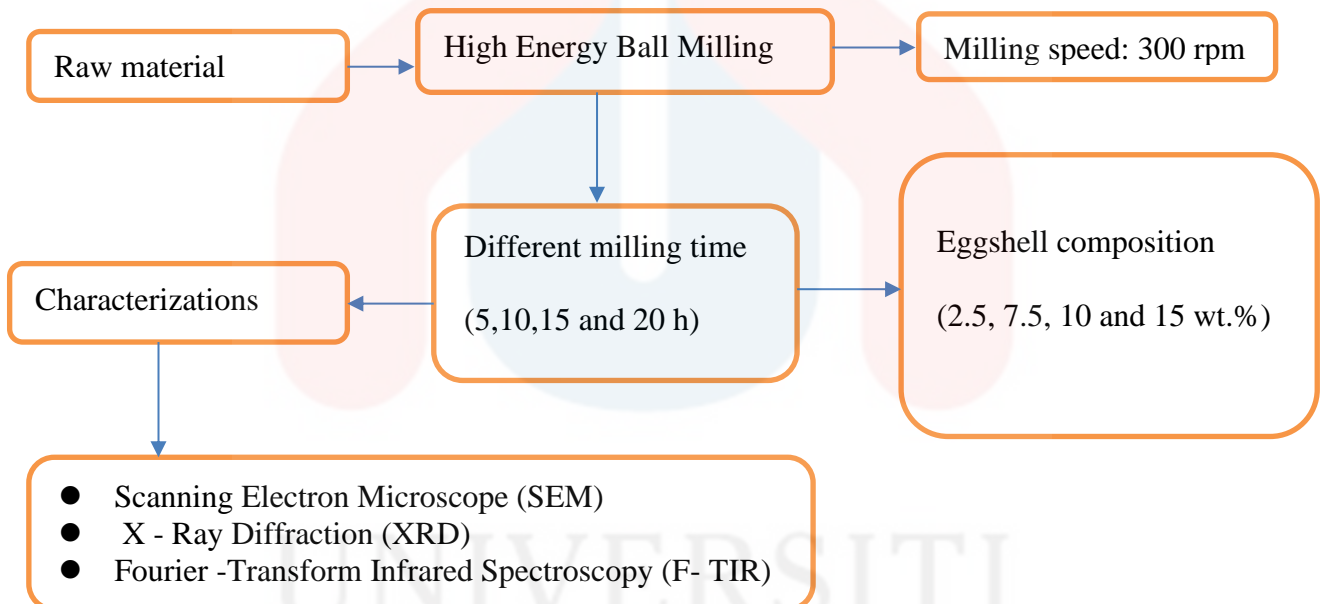


Figure 3.1: Overall experiment in this study

3.2 Raw Material

Raw material that will be used in this study are Al_2O_3 ($\geq 98\%$ purity, 70% volume, average particle size $> 20 \mu\text{m}$ powder, TiO_2 ($> 99.5\%$ purity, average particle size $> 21\text{nm}$) and will be purchased from Sigma Aldrich. The chicken eggshell used in this study will be obtained from a local store.

3.3 Composition Preparation

The composition of Al_2O_3 - TiO_2 nanocomposite was calculated using the rule of mixture.

From rule of mixture equation,

$$\text{Wt}\% = \frac{\text{mass of powder}}{\text{total mass of powder}} \times 100\%$$

Where, mass of the powder is Al_2O_3 or TiO_2 - eggshell while total mass of powder is the total mass of Al_2O_3 plus TiO_2 - eggshell,

$$\text{Wt.}\% = \frac{70g(\text{mass of Al}_2\text{O}_3)}{100g} \times 100\% \quad (3.1)$$

$$= 70 \text{ g}$$

$$\text{Wt.}\% = \frac{30g(\text{mass of TiO}_2\text{-ES})}{100g} \times 100\% \quad (3.2)$$

$$= 30 \text{ g}$$

Where from the calculation Al_2O_3 is 70 g as shown in (3.1) and TiO_2 - ES is 30 g shown in (3.2).

Table 3.1: Conversion table for the sample

Sample	Represent
TAE-0.5G-5H	TAE-2.5wt%-5H
TAE-0.5G-10H	TAE-2.5wt%-10H
TAE-0.5G-15H	TAE-2.5wt%-15H
TAE-0.5G-20H	TAE-2.5wt%-20H
TAE-1.5G-5H	TAE-7.5wt%-5H
TAE-1.5G-10H	TAE-7.5wt%-10H
TAE-1.5G-15H	TAE-7.5wt%-15H
TAE-1.5G-20H	TAE-7.5wt%-20H
TAE-2G-5H	TAE-10wt%-5H
TAE-2G-10H	TAE-10wt%-10H
TAE-2G-15H	TAE-10wt%-15H
TAE-2G-20H	TAE-10wt%-20H
TAE-3G-5H	TAE-15wt%-5H
TAE-3G-10H	TAE-15wt%-10H
TAE-3G-15H	TAE-15wt%-15H
TAE-3G-20H	TAE-15wt%-20H

3.3.1 Preparation of the eggshell powder

The ES was obtained from the local entrepreneur. The collected ES waste was washed with distilled water for 3 until 4 times and then let dry in the sun until completely dry. The dry ES was roughly crushed into small pieces and then grinded with the mortar to become the powder form. The ES powder will be sieved with a 125-micron meter sieve and then placed in an oven at a temperature of 100 degrees Celsius for 24 hours..

Figure 3.2: Oven



3.3.2 High Energy Milling

The milling was performed in a planetary ball mill with a constant speed of 300 rpm at different time intervals: 5, 10, 15, and 20 hours. Zirconia balls with a diameter of 5 mm were used in the milling process.

Scanning Electron Microscopy (SEM) was employed to examine and image the surface of the samples. In the SEM, a concentrated electron beam was directed at the sample, and the interaction between the high-energy electrons and the sample's atoms generated various signals. After the detection and processing of these signals, a highly accurate and three-dimensional image of the sample surface was created.



Figure 3.3: High energy planetary ball mill

UNIVERSITI
MALAYSIA
KELANTAN

3.4 Characterisation of Al₂O₃-TiO₂-ES Nanocomposites

3.4.1 X-Ray Diffraction (XRD)

The structural characteristics, phase identification, and parameter impact on the alumina-titania-eggshell nanocomposite were determined using the X-ray diffraction technique (XRD, Bruker D2 Phaser). The XRD pattern of the alumina, titania, and eggshell nanocomposite will analyze using Software DIFRACE.EVA for phase identification. With a 2θ angle between 20° and 90° , the step size will always be set at 0.02° . From the XRD peak pattern, it is possible to determine the crystalline size and internal strain. The Williamson-Hall (WH) technique, which is frequently used to assess the crystallite size and internal strain of milled composite powder, will then be used to measure the crystallize size and internal size strain. B is equivalent to the entire widening of size, lattice strain, and instrument when full line broadening is assuming.

$$B_o = B_i - B_{crys} + B_{strain} \quad (3.3)$$

Where B_i broadening due to the instrumental, B_{crys} broadening cause by crystallite size and B_{strain} broadening cause by strain. After subtracting the instrument effect from Equation 3.1:

$$B_r = B_{crys} + B_{strain} \quad (3.4)$$

Where B_r refer to the overall broadening after eliminates the instrument broadening. Therefore, according to Williamson & Hall (1953), the WH method will be as (3.3) since only crystallite size and internal strain that left.

$$B_r \cos \theta = \frac{k\lambda}{D} + \eta \sin \theta \quad (3.5)$$

Where η refer to internal strain, B_r refer to crystallite size, λ refer to wavelength of the X-ray, θ is the Bragg angle, k is 0.89.

3.4.2 Fourier -Transform Infrared Spectroscopy (F-TIR)

By observing the interaction between the sample and infrared light, the Fourier - Transform Infrared Spectroscopy (F-TIR) is a potent analytical tool that may be used to ascertain the chemical makeup of a sample. This test is non-destructive and is the technique used to both detect and identify unidentified material while also providing a complete study of the functional group in the sample at hand. Infrared light is sent through the sample in this method, and the quantity of absorption at various frequencies is then measured. To identify the various functional groups in the sample, the result will be displayed on a graph by plot with the absorbance at each frequency. The infrared absorptivity versus frequency plot, with peaks corresponding to the sample's absorption of infrared light, will demonstrate the outcome from the F-TIR spectra.

CHAPTER 4

RESULTS AND DISCUSSION

4.1 Raw Material

4.1.1 Phase Identification

Figure 4.1 shows the XRD patterns of Al_2O_3 , TiO_2 and ES. The Al_2O_3 peaks show out the few obvious peaks which are at 26.4° , 35.5° , 43.4° , 58.6° , but for the ES peaks, there is only one highest peak that is clearly shown which is at 59.5° . The peaks 26.4° , 27.1° , 46.4° are assigned as TiO_2 .

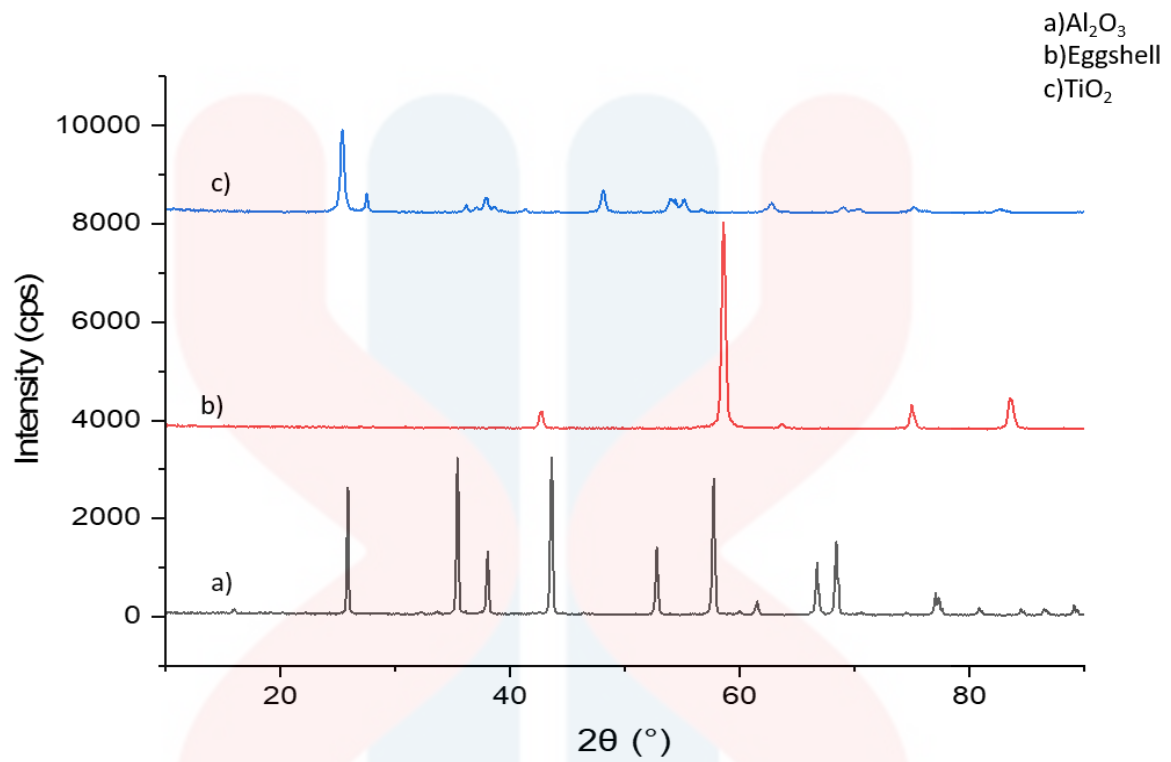


Figure 4.1: XRD pattern of the raw material Al_2O_3 , TiO_2 , ES

UNIVERSITI
MALAYSIA
KELANTAN

4.1.2 Functional Group

The raw ES FTIR spectrum is shown in Figure 4.2. The O-H stretching vibration region is represented by the peak at 3642 cm^{-1} , which is associated with the bond of CaO at 1790 cm^{-1} and 1504 cm^{-1} on the surface (Puspitasari et al., 2020). The Ca-Co group was generated by the ES in the $1405\text{--}873\text{--}712\text{ cm}^{-1}$ range. The wave numbers 1405 cm^{-1} , 873 cm^{-1} , and 712 cm^{-1} , respectively, represent in-plane bending, out-of-plane bending, and anasymmetric stretching regions (Cahya & Marfuah, 2014). According to Rohimet al. (2014), the functional group of eggshells exhibits the Ca-O bond at 670 cm^{-1} , showing that CaO was totally changed from CaCO_3 .

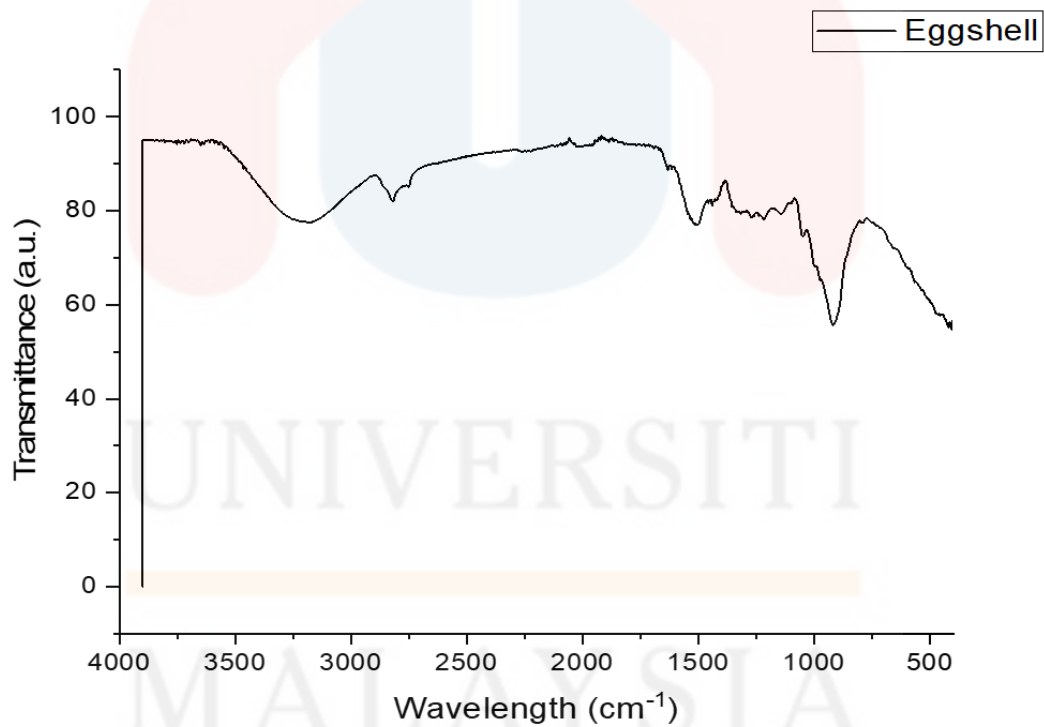


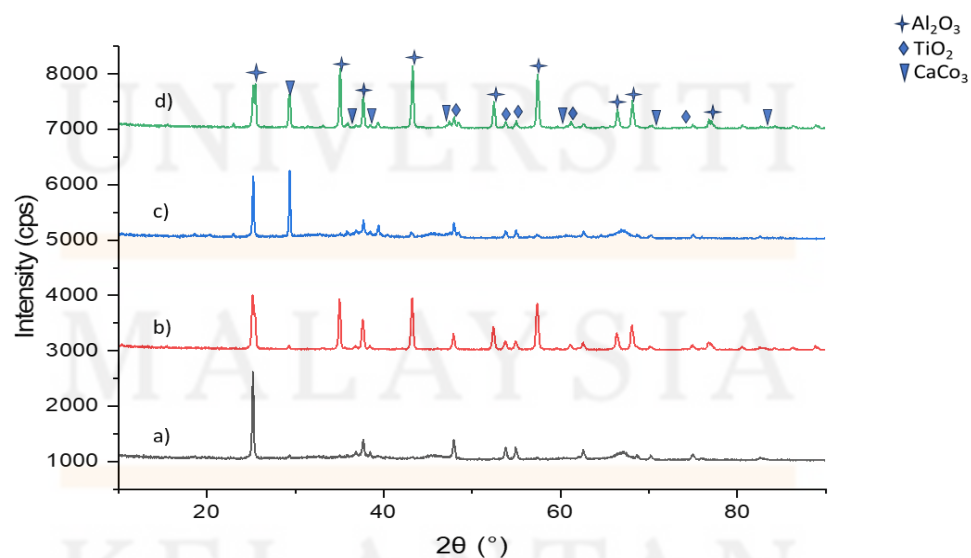
Figure 4.2: FTIR pattern of the raw material eggshell

4.2 Al₂O₃-TiO₂-ES Nanocomposite

4.2.1 Phase Identification

Figure 4.3 shows the XRD patterns of the as-milled Al₂O₃-TiO₂-ES nanocomposite at different ES compositions and milling times. All the powder mixtures that were identified consist of more than one crystalline phase, each with varying degrees of intensity. The most intense peaks at 25.4°, 35.1°, 38.5°, 40.4°, 54.6°, 68.2° are determined as Al₂O₃ (COD 9009671). These peaks become slightly broadened with the addition of a higher amount of ES (15wt%) at higher milling time (20 h). A similar observation can also be seen for the TiO₂ peaks (COD 5000223). The widening of the peaks at greater milling times is produced by increased deformation from collision occurrences, which results in more structural refinement than at lower milling times. The probability of stacking faults and dislocation density increases with milling time, leading to a nanostructure.

The appearance of the CaCO₃ from raw ES clearly shows the peaks at 29.4°, 35.8°, 39.4°, 47.4°, 60.6°, 70.2° and 81.5° (COD 1010962). The presence of other phases from reaction of CaCO₃ and Al₂O₃, TiO₂ was not detected. However, it has been determined that there is a deposition of TiO₂ covering the surface of CaCO₃ (Onwubu et al.,



2019).

Figure 4.3: XRD pattern of the milled powder mixture for a)2.5wt%-5h, b)2.5wt%-20h, c)15wt%-5h and 15wt%-20h milled at 300 rpm

4.2.2 Crystallite size and internal strain

The Al_2O_3 crystallite size and internal strain was used by the Williamson Hall (WH) method. Figure 4.4 shows the plot of $B_r \cos \theta$ against $\sin \theta$ derived from WH method. The slope reveals the internal strain, while the y-intercept indicates the crystallite size. A negative slope value means larger crystallites and less internal strain.

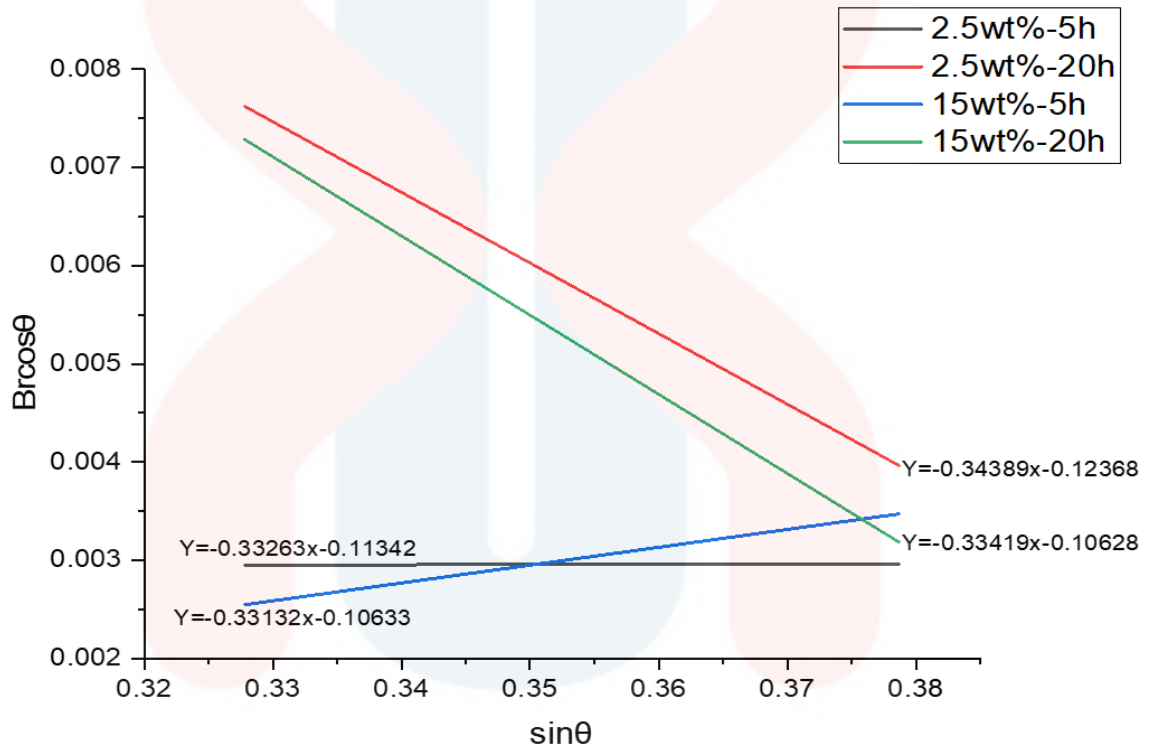


Figure 4.4: Plot of $B_r \cos \theta$ against $\sin \theta$ for calculating Al_2O_3 crystallite size and internal strain at different ES compositions and milling time using WH method

Figure 4.5 shows the Al_2O_3 crystalline size and internal strain at different ES compositions and milling times. The size of the crystallites reduces dramatically after 20 hours of milling, from 5 hours. This decreasing crystallite size indicates that longer milling times produce smaller crystallite sizes or finer particles. Increased mechanical forces and the material's refining during milling may be to blame for this. As the milling time rises, the strain shifts from positive (tensile) to negative (compressive). Expanding is indicated by a positive strain, and compressing is shown by a negative strain. This implies that during milling, the material gets compressed, and it causes more milling power.

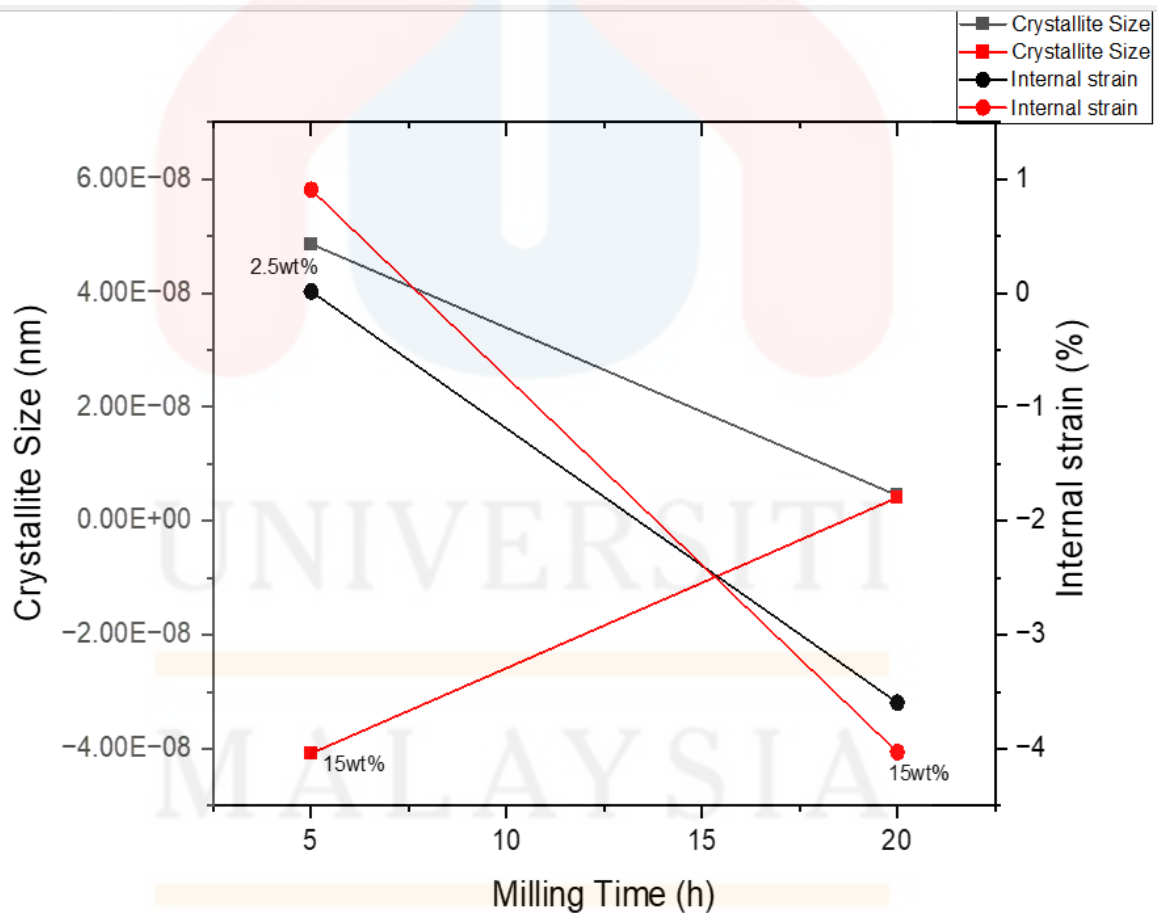


Figure 4.5: Crystallite size and internal strain of the milled powder with different ES composition and milling times

4.2.3 Functional group

FTIR spectroscopy analysis was conducted to identify the presence of any functional group in Al_2O_3 - TiO_2 -ES nanocomposite. Figure 4.6 shows the FTIR spectra of Al_2O_3 - TiO_2 -ES nanocomposite at different ES compositions milled for 10 h. Based on the figure, the aliphatic C-H stretching area is represented by a large peak in the infrared range between 2500 and 2250 cm^{-1} . The peak relates to the stretching vibration of aliphatic (non-aromatic) C-H bonds, which is typically wide. The wide peak at 1550-1400 cm^{-1} is attributed to C-N stretching, and the functional group of this peak was detected in the range when the sample included nitrogen-containing chemicals, such as amines or amides. The peak from 650 to 500 cm^{-1} corresponds to Al-O and Ti-O, or metal-oxygen stretching. Stretching vibrations involving metal-oxygen bonds can occur in this range. The carbonate group might be seen as wide bands between 700 and 600 cm^{-1} due to vibration caused by CaCO_3 or another mineral component. Furthermore, the second component, an ES component, may be measured at less than 500 cm^{-1} .

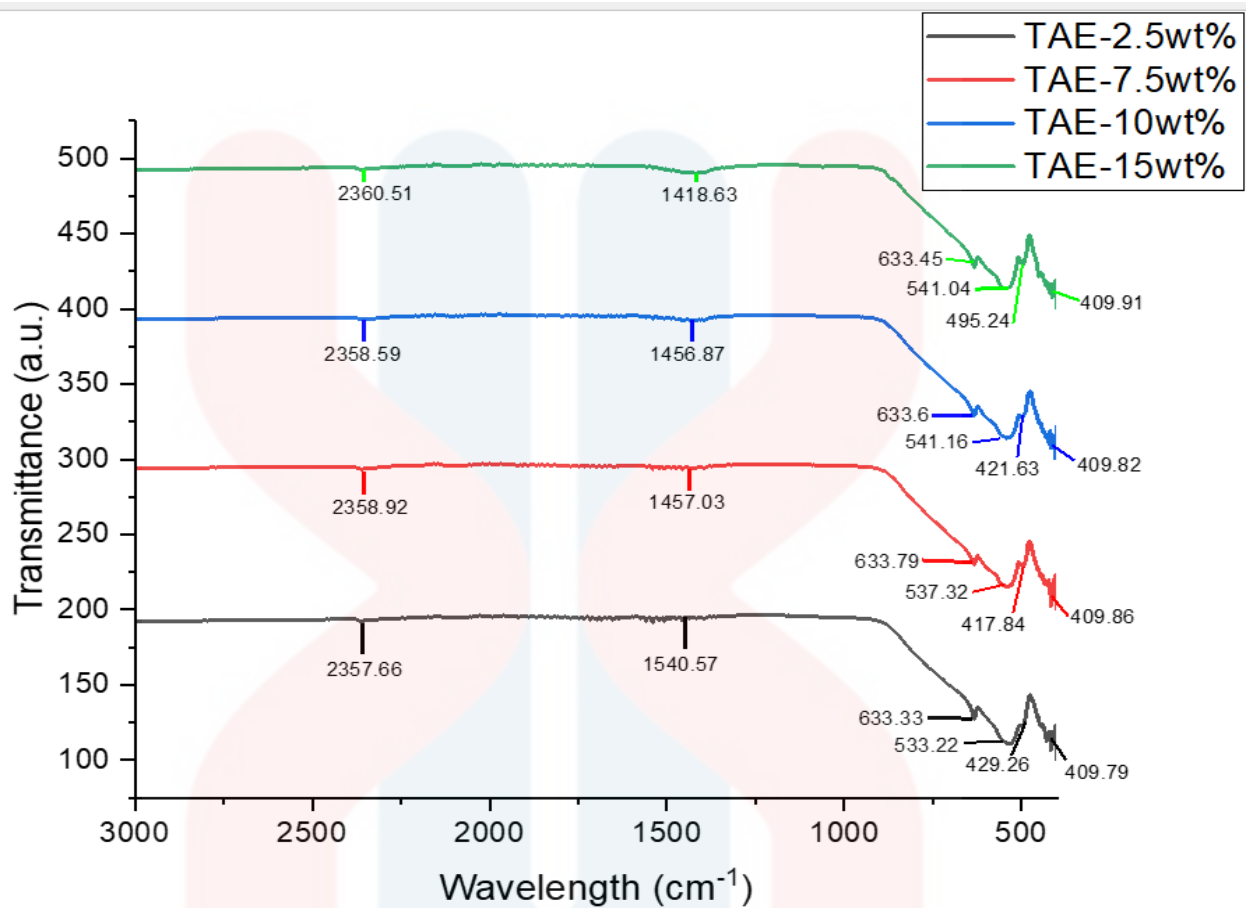


Figure 4.6: FTIR pattern of the milled powder mixture at the different composition for 10h milling time

For the figure 4.7, the FTIR spectra of the nanocomposite powder for 20h milling time have shown from the broad peak. The broad peak at 2500cm^{-1} to 2250cm^{-1} in the infrared region corresponds to the aliphatic C-H stretching region. So, in this range, the observation about the peak is associated with the stretching vibration of aliphatic (non-aromatic) C-H bonds and this peak is usually broad. The broad peak at $1550 - 1400\text{cm}^{-1}$ are assigned C-N stretching and the functional group of this peak has been observed at the range which the sample was containing nitrogen-containing compounds, such as amines or amides. The peak from $650 - 500\text{cm}^{-1}$ assigned Al-O and Ti-O or metal-oxygen stretching. Metal oxides such as alumina and titania, stretching vibrations involving metal-oxygen bonds can occur in this range((Lefèvre, 2004)). The carbonate group could be observed appear as broad bands between $700 - 600\text{ cm}^{-1}$ due to vibration associated with CaCO_3 or another mineral component ((Legodi et al., 2001)). In addition, the second component is an ES component that can determine below 500 cm^{-1} .

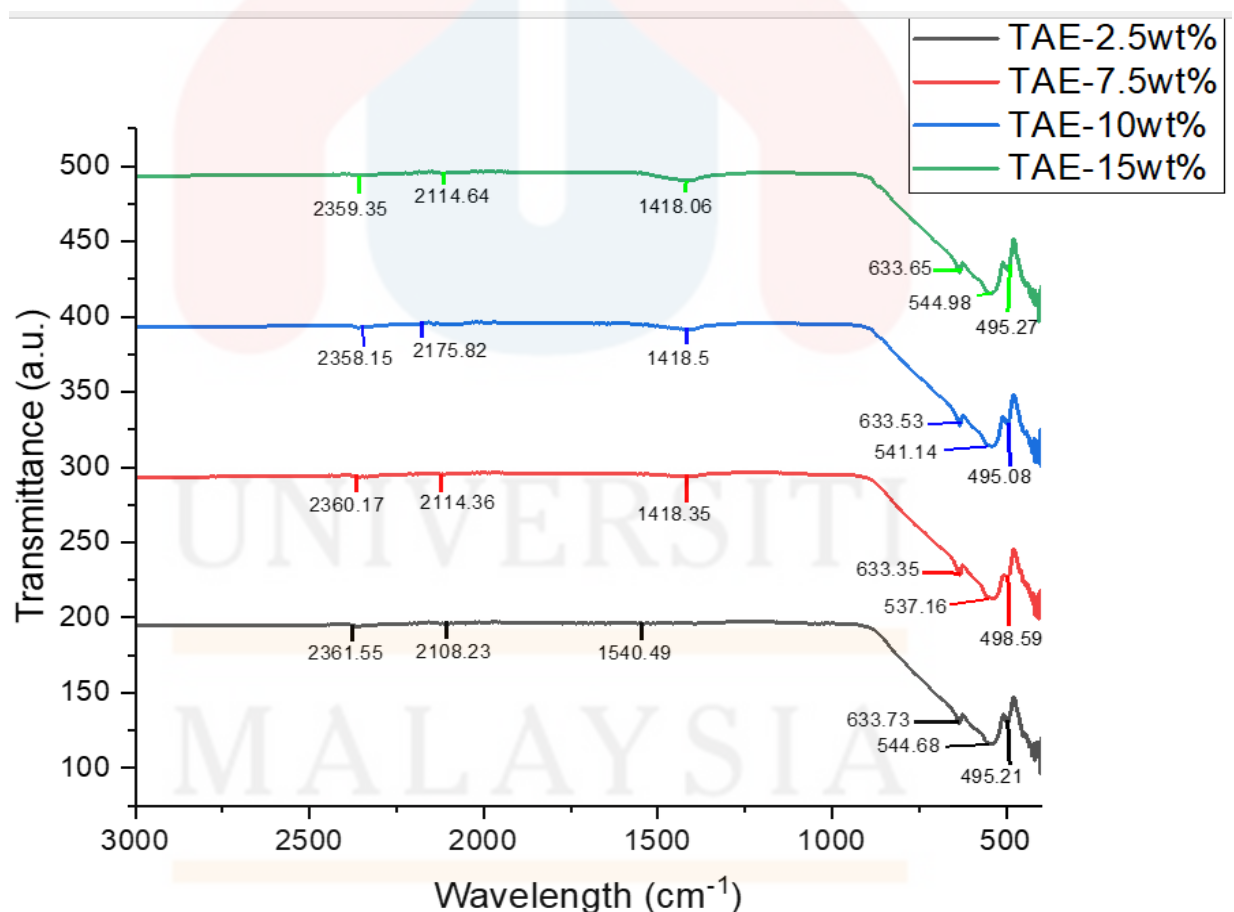


Figure 4.7: FTIR pattern of the milled powder mixture at the different ES composition milled for 20h

4.3 Morphology

The morphology of Al_2O_3 - TiO_2 -ES nanocomposite at different ES composition and milling time was captured using scanning electron microscope (SEM) is shown in Figures 4.8 for 500x magnification. Figures 4.8 demonstrate the morphological development of milled powder at 300 rpm across varied milling times. During all milling periods, the microstructure is made up of evenly distributed particles of all shapes and sizes. The image a from figure 4.8 which is sample for 2.5wt% eggshell composition and 5 hour milling time has been detected in 500x magnification, from the image has shown the milled powder sample was combine into one cubic structure which the outside layer was coating with the TiO_2 , and the cubic structure is the Al_2O_3 element. For the part of the eggshell powder was show out by plush form that mix with the TiO_2 at the Al_2O_3 outside layer. The image b was the same type as sample a, but the difference is the milling time was increase to 20 hours. It was shown that the milled powder sample has become overly fragmented and unable to be completely classified and detected. The image c milled powder sample was different from the eggshell composition which is increase to 15wt%. The image shows the structure of the powder, which is like image a, but the plush form of the eggshell powder is easier to detect. For image d, the particle similar like image b which the particle is become uneven crushing pattern.

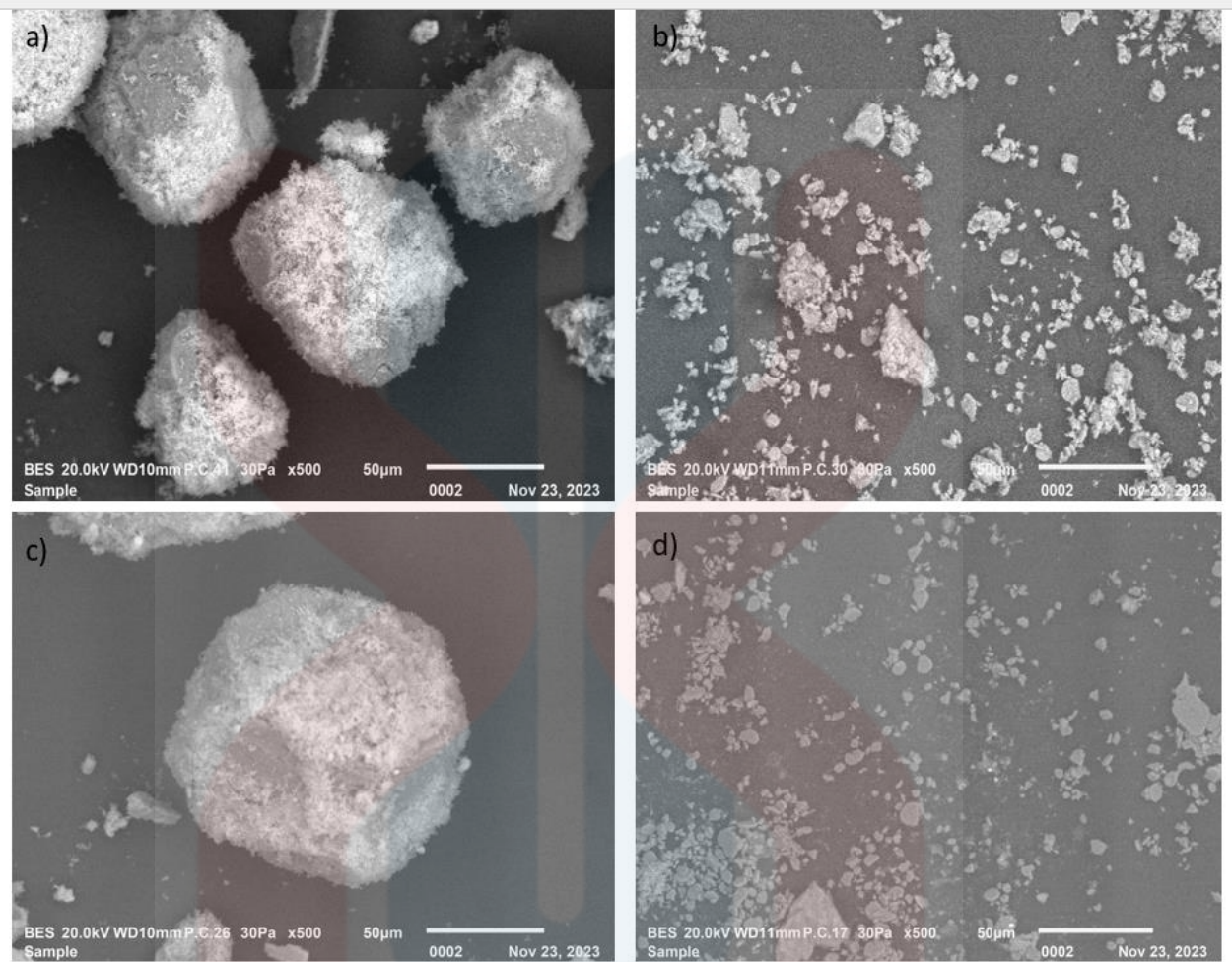


Figure 4.8: SEM images of Al_2O_3 - TiO_2 - Eggshell powder milled at (a) 2.5wt%-5h (b) 2.5wt%-20h (c) 15wt%-5h (d) 15wt%-20h at 300 rpm at 500x magnification

CONCLUSIONS AND RECOMMENDATIONS

5.1 Conclusions

In this study, the preparation Al_2O_3 - TiO_2 -ES nanocomposite by powder metallurgy was successfully achieved. The microstructure and properties of the Al_2O_3 - TiO_2 -ES that use high energy ball milling was evaluated by using scanning electron microscope (SEM), Fourier -Transform Infrared Spectroscopy (F-TIR), X-Ray Diffraction (XRD). The conclusion retrieved from this study are:

1. Difference in milling time and composition of ES affects the microstructure, structural and functional group of Al_2O_3 - TiO_2 -ES nanocomposites.
2. Increasing the milling time produced finer and less agglomerated Al_2O_3 - TiO_2 -ES morphology and particle size due to enhancement deformation from high impact energy.
3. The peak intensity of XRD pattern will reduce as the milling time elongates and cause the decreasing in crystalline size.

5.2 Recommendations

It has been acknowledged that by altering the PM parameters, it can change the nature of microstructure and properties of the nanocomposites. The first suggestion would be to do is analysis of the raw material or the raw powder before this study being carried out. This will help in giving out a better result for doing the comparison with the initial morphology, shape, and average size of the powder.

Next is doing the characterization testing such as brunauer-emmett-teller (BET) analysis on the sample to study information on their physical structure as the area of a material's surface affects when interact to nitrogen gasses and do some mechanical testing after the compaction to study impact of milling time of the nanocomposite to calculate the green density testing.

Last recommendation is observed the microstructural and the properties of the sample after the sintering test if the time is enough.

REFERENCES

- Al-Oqla, F. M., Sapuan, S., Anwer, T., Jawaid, M., & Hoque, M. (2015). Natural fiber reinforced conductive polymer composites as functional materials: A review. *Synthetic Metals*, 206, 42-54.
- Alves, M. F., dos Santos, C., Cossu, C. M., Suzuki, P. A., Ramos, A. S., Ramos, E. C., Simba, B. G., & Strecker, K. (2020). Development of dense Al₂O₃–TiO₂ ceramic composites by the glass-infiltration of porous substrates prepared from mechanical alloyed powders. *Ceramics International*, 46(2), 2344-2354.
- Essabir, H., Bensalah, M., Rodrigue, D., Bouhfid, R., & Qaiss, A. (2016). Structural, mechanical and thermal properties of bio-based hybrid composites from waste coir residues: Fibers and shell particles. *Mechanics of Materials*, 93, 134-144.
- Hassan, S., & Aigbodion, V. (2015). Effects of eggshell on the microstructures and properties of Al–Cu–Mg/eggshell particulate composites. *Journal of King Saud University-Engineering Sciences*, 27(1), 49-56.
- Hassan, S., Aigbodion, V., & Patrick, S. (2012). Development of polyester/eggshell particulate composites. *Tribology in industry*, 34(4), 217.
- Jang, K.-S. (2016). Mineral filler effect on the mechanics and flame retardancy of polycarbonate composites: Talc and kaolin. *e-Polymers*, 16(5), 379-386.
- Karadimas, G., & Salonitis, K. (2023). Ceramic Matrix Composites for Aero Engine Applications—A Review. *Applied Sciences*, 13(5), 3017.
- Kim, Y. W., & Lee, J. G. (1989). Pressureless Sintering of Alumina-Titanium Carbide Composites. *Journal of the American Ceramic Society*, 72(8), 1333-1337.

- Lefèvre, G. (2004). In situ Fourier-transform infrared spectroscopy studies of inorganic ions adsorption on metal oxides and hydroxides. *Advances in colloid and interface science*, 107(2-3), 109-123.
- Legodi, M., De Waal, D., Potgieter, J., & Potgieter, S. (2001). Rapid determination of CaCO₃ in mixtures utilising FT—IR spectroscopy. *Minerals Engineering*, 14(9), 1107-1111.
- Meneghetti, P., & Qutubuddin, S. (2006). Synthesis, thermal properties and applications of polymer-clay nanocomposites. *Thermochimica acta*, 442(1-2), 74-77.
- Nurdina, A., Mariatti, M., & Samayamutthirian, P. (2009). Effect of single-mineral filler and hybrid-mineral filler additives on the properties of polypropylene composites. *Journal of Vinyl and Additive Technology*, 15(1), 20-28.
- Onwubu, S. C., Mdluli, P. S., Singh, S., Madikizela, L., & Ngombane, Y. (2019). Characterization and in vitro evaluation of an acid resistant nanosized dental eggshell-titanium dioxide material. *Advanced Powder Technology*, 30(4), 766-773.
- Paul, R., Gouda, K., & Bhowmik, S. (2021). Effect of Different constraint on tribological behaviour of natural fibre/filler reinforced polymeric composites: A review. *Silicon*, 13(8), 2785-2807.
- Pinzón, A. V., Urrego, K. J., González-Hernández, A., Ortiz, M. R., & Galvis, F. V. (2018). Corrosion protection of carbon steel by alumina-titania ceramic coatings used for industrial applications. *Ceramics International*, 44(17), 21765-21773.
- Rathod, V. T., Kumar, J. S., & Jain, A. (2017). Polymer and ceramic nanocomposites for aerospace applications. *Applied Nanoscience*, 7, 519-548.

- Roy, K., Pongwisuthiruchte, A., Debnath, S. C., & Potiyaraj, P. (2021). Application of cellulose as green filler for the development of sustainable rubber technology. *Current Research in Green and Sustainable Chemistry*, 4, 100140.
- Sharma, A., Aravindhana, S., & Krishnamurthy, R. (2001). Microwave glazing of alumina–titania ceramic composite coatings. *Materials Letters*, 50(5-6), 295-301.
- Sunardi, S., Ariawan, D., Surojo, E., Prabowo, A. R., Akbar, H. I., Cao, B., & Carvalho, H. (2023). Assessment of eggshell-based material as a green-composite filler: Project milestones and future potential as an engineering material. *Journal of the Mechanical Behavior of Materials*, 32(1), 20220269.
- Vandeginste, V. (2021). Food waste eggshell valorization through development of new composites: A review. *Sustainable Materials and Technologies*, 29, e00317.
- Zaaba, N. F., & Ismail, H. (2019). Thermoplastic/Natural Filler Composites: A Short Review. *Journal of Physical Science*, 30.

APPENDIX A



UNIVERSITI

MALAYSIA

KELANTAN

APPENDIX B



UNIVERSITI

MALAYSIA

KELANTAN

APPENDIX C



UNIVERSITI

MALAYSIA

KELANTAN